Ecological Applications, 0(0), 2018, pp. 1–11
© 2018 The Authors. *Ecological Applications* published by Wiley Periodicals, Inc. on behalf of Ecological Society of America.
This is an open access article under the terms of the Creative Commons Attribution License, which permits use, distribution and reproduction in any medium, provided the original work is properly cited.

Assessing the effectiveness of Landsat 8 chlorophyll *a* retrieval algorithms for regional freshwater monitoring

Jonah Boucher,[1] Kathleen C. Weathers,[2,4] Hamid Norouzi,[3] and Bethel Steele[2]

[1]*Hamilton College, Clinton, New York 13323 USA*
[2]*Cary Institute of Ecosystem Studies, Millbrook, New York 12545 USA*
[3]*Earth and Environmental Sciences, The Graduate Center, City University of New York, New York, NY 10016 USA*

Abstract. Predicting algal blooms has become a priority for scientists, municipalities, businesses, and citizens. Remote sensing offers solutions to the spatial and temporal challenges facing existing lake research and monitoring programs that rely primarily on high-investment, in situ measurements. Techniques to remotely measure chlorophyll *a* (chl *a*) as a proxy for algal biomass have been limited to specific large water bodies in particular seasons and narrow chl *a* ranges. Thus, a first step toward prediction of algal blooms is generating regionally robust algorithms using in situ and remote sensing data. This study explores the relationship between in-lake measured chl *a* data from Maine and New Hampshire, USA lakes and remotely sensed chl *a* retrieval algorithm outputs. Landsat 8 images were obtained and then processed after required atmospheric and radiometric corrections. Six previously developed algorithms were tested on a regional scale on 11 scenes from 2013 to 2015 covering 192 lakes. The best performing algorithm across data from both states had a 0.16 correlation coefficient (R^2) and $P \leq 0.05$ when Landsat 8 images within 5 d, and improved to R^2 of 0.25 when data from Maine only were used. The strength of the correlation varied with the specificity of the time window in relation to the in-situ sampling date, explaining up to 27% of the variation in the data across several scenes. Two previously published algorithms using Landsat 8's Bands 1–4 were best correlated with chl *a*, and for particular late-summer scenes, they accounted for up to 69% of the variation in in-situ measurements. A sensitivity analysis revealed that a longer time difference between in situ measurements and the satellite image increased uncertainty in the models, and an effect of the time of year on several indices was demonstrated. A regional model based on the best performing remote sensing algorithm was developed and was validated using independent in situ measurements and satellite images. These results suggest that, despite challenges including seasonal effects and low chl a thresholds, remote sensing could be an effective and accessible regional-scale tool for chl a monitoring programs in lakes.

Key words: *chl* a; *eutrophication; in situ measurements; Landsat; remote sensing; small lakes.*

Introduction

Scientists and citizens alike are becoming increasingly interested in monitoring and predicting changes in global water quality (Hanson et al. 2016). Freshwater systems, in particular, provide a wide range of ecosystem services, from habitats to recreation to irrigation, and are undergoing major changes (Stoddard et al. 2016). Environmental stressors related to climate and land-use change are threatening many of these services, leading public and private organizations to rejuvenate or begin monitoring strategies. Many such efforts have begun in response to anthropogenic eutrophication from increasing nutrient inputs and higher water temperatures that are changing freshwater biota community dynamics (Dörnhöfer and Oppelt 2016). The effects of eutrophication can range from aesthetic annoyances such as odor and color to toxic blooms that decimate wildlife populations and make the water unsuitable to drink (Shen et al. 2012). Monitoring programs have thus aimed to predict phytoplankton population change with the hope of predicting and, ultimately, preventing these problematic situations.

While in situ, and primarily summer time, measurements have long been the basis of lake monitoring programs, sampling is often limited in space and time because of the high time and labor costs of data collection. An alternative, or complement, to in situ approaches uses remote sensing technology, from which satellite imagery data can be used to derive water quality parameters. Remote sensing has shown promise for supplementing or replacing field data, but limited spatial resolution and optically complex inland waters have posed challenges to progress (Palmer et al. 2015).

Recent advances in the remote sensing technology and data accessibility have the potential to overcome some historic challenges. Landsat 8 is the most recent addition to the Landsat series of satellites, which have provided a publically accessible record of over four million images dating back to 1972. Landsat 8 features eight times better signal-to-noise ratio than previous iterations, a faster 12-bit quantization processing speed, and two new wavelengths (Roy et al. 2014). Although the 16-d repeat cycle of the satellite results in temporal limitations, the 30 × 30 m spatial resolution has made Landsat 8 one of the most promising versions of remote sensing technology yet for inland water monitoring (Gerace et al. 2013, Feyisa et al. 2014, Beck et al. 2016,

Manuscript received 27 June 2017; revised 23 December 2017; accepted 2 January 2018. Corresponding Editor: David S. Schimel.
[4] E-mail: weathersk@caryinstitute.org

Concha and Schott 2016, Urbanski et al. 2016). The applicability of Landsat 8 satellite data remains to be fully tested, however.

The application of remote sensing to monitoring water quality is limited to measuring spectrally active water parameters, since these satellites can only produce data about absorbance and reflectance of surfaces. However, the issue of eutrophication of lakes has potential to be investigated with remote sensing due to the fact that chlorophyll *a* (chl *a*) is a spectrally active compound in phytoplankton. Chl *a* can be used as a proxy for phytoplankton biomass, therefore serving as an indicator of lake productivity (Beck et al. 2016). Over the past several years, many different algorithms have been developed to estimate chl *a* values from reflectance outputs of specific bands from satellite data. Robust relationships have been developed in many cases (Duan et al. 2007, Bresciani et al. 2011, Keith et al. 2012, Tebbs et al. 2013) between measured and satellite-retrieved chl *a* values, but their application is not necessarily accurate outside of the original area of study (Moses et al. 2012) and season (Liga et al. 2017).

Lakes in the New England region have long been monitored using traditional in situ methods. The Volunteer Lake Assessment Program (VLAP) has used volunteer-driven lake sampling sponsored by the Department of Environmental Services to monitor New Hampshire lakes since 1985. The organization is currently collecting monthly water samples and compiling annual reports on 176 different lakes in the state (New Hampshire Department of Environmental Services 2015). Likewise, the Volunteer Lake Monitoring Program in Maine, with the help of over 1,200 active volunteers, has been monitoring more than 500 lakes since 1971 (Maine Volunteer Lake Monitoring Program 2017). Of primary concern to the managers, citizens, and scientists alike is eutrophication, and associated algal blooms, which are expected to be growing problems in the region due to nutrient loading from land-use and climate change (Moore et al. 2014). Studies on lakes in the region have largely been limited to in situ case studies on specific lakes (Davis et al. 2006, Carey et al. 2009) and the use of remote sensing technology for regional monitoring has not been fully explored.

Monitoring small oligotrophic lakes remotely was suggested as early as 1989 (Vertucci and Likens 1989), but limitations on the resolution and accuracy of remote sensing technology precluded any further action at the time. In New Hampshire, early Landsat data were used to examine the relationship between satellite reflectance and lake transparency, but were limited by the band availability of Landsat (Schloss et al. 2002). More recent work has identified remote sensing of chl *a* as a priority, but has used hyperspectral imaging from boats or aircraft rather than available satellite imagery (U.S. EPA 2010, Keith et al. 2012). Urbanski et al. (2016) provided an initial assessment of Landsat 8's suitability for regional lake quality assessment, finding that remote sensing for trophic state assessment of lakes in Poland was possible, but often required a specific formula for each specific satellite scene. Here we utilize the currently available in situ and satellite data across New Hampshire and Maine to assess the strength of existing chl a retrieval algorithms and their potential as monitoring tools across the region.

Data and Methods

Satellite data

Five Landsat images over Maine (Path 12 Row 29) and seven over New Hampshire (Path 13 Row 30) were acquired from USGS EarthExplorer (Table 1; data *available online*[5]). The Level 1 GeoTIFF Data Products from the Landsat 8 OLI_TIRS sensor were downloaded for each image, except for the 26 August 2000 image, which instead came from Landsat 7's Level 1 product and was used to provide a comparison between Landsat iterations (Appendix S1: Table S1). The images were processed using ENVI software (Harris Geospatial, Broomfield, Colorado, USA). For each of Landsat 8's 11 different bandwidths (Appendix S1: Table S1) reflective radiometric calibration was performed to convert radiance, the surface brightness measured directly by the satellite, to the unitless surface reflectance using metadata about the acquisition time and sun elevation when the image was taken (Harris Geospatial Broomfield, Colorado, USA). A simple dark object subtraction (DOS) was performed to minimize the effects of atmospheric haze (Giardino et al. 2001, Urbanski et al. 2016). Dark object subtraction searches each band for the darkest pixel value. Assuming that dark objects reflect no light, any value greater than zero must result from atmospheric scattering. The scattering is removed by subtracting this value from every pixel in the band. This method is primarily effective for haze correction in multispectral data (Harris Geospatial).

In situ data

In situ chl *a* data were obtained for New Hampshire from the Department of Environmental Service's Volunteer Lake Assessment Program (VLAP) database and for Maine from the Volunteer Lake Monitoring Program (VLMP; Fig. 1). In total, 351 chl *a* samples were taken from 260 unique sampling points in 192 different lakes (131 in Maine and 61 in New Hampshire; Table 1). Any pair of scenes in Maine had on average 15 sampling points in common and no more than 23, and in New Hampshire any pair had on average fewer than three points in common and no more than six.

Chl *a* measurements taken from lakes within the satellite image and sampled within five days for New Hampshire images and five days for Maine images were recorded. Chl *a* samples were taken from depths ranging from 0.5 to 10 m depending on the lake (data *available online*).[6,7] Reported sample locations (latitude and longitude) were matched spatially with the USGS National Hydrography Dataset best resolution files (U.S. Geological Survey, National Geospatial Program, 2017*a,b*) using ESRI ArcMap 10.4 (ESRI, Redlands, California, USA) to extract lake area statistics. Lakes in Maine had a median area of 100 ha (0.6–4,500 ha range) and New Hampshire lakes had a median area of 62 ha (2.3–1,700 ha range). In situ chl *a* data were natural-log-transformed in our analyses because of their non-

[5] https://earthexplorer.usgs.gov/
[6] www.mainevlmp.org
[7] www.des.nh.gov/organization/divisions/water/wmb/vlap/

TABLE 1. Landsat 8 images acquired over Maine (P12R29) and over New Hampshire (P13R30). The available corresponding in situ chl *a* lake data are from Maine and New Hampshire, USA volunteer water monitoring programs.

Date	Sampling points	Unique lakes	Chl *a*			Lakes with chl *a* > 10 µg/L
			Minimum	Maximum	Median	
New Hampshire						
12 July 2013	19	19	1.41	11.05	4.75	2
30 September 2013	2	2	5.65	5.73	5.69	0
29 June 2014	13	13	1.29	6.74	3.76	0
17 September 2014	5	4	1.79	6.55	2.59	0
3 October 2014	6	3	1.32	9.51	2.54	0
3 August 2015	17	17	1.55	12.1	3.28	2
19 August 2015	28	25	1.07	9.77	2.53	0
Maine						
26 August 2000†	69	56	1.2	48.4	4.4	11
19 June 2013	19	15	1.3	48	3.0	1
22 August 2013	64	54	1.3	56	3.2	4
9 August 2014	52	43	1.2	17	3.9	3
25 August 2014	57	51	1.2	65	4.4	11

†26 August 2000 is from Landsat 7 (Appendix S2: Fig. S1).

normal distribution (Kabbara et al. 2008, Watanabe et al. 2015, Urbanski et al. 2016).

Assessing algorithm performance

Six existing chl *a* retrieval algorithms were chosen to incorporate several different potentially ecologically relevant bandwidths (Table 2). The Surface Algal Bloom Index (SABI) and Normalized Difference Vegetation Index (NDVI) were developed for satellites with narrower bandwidths and were adapted to fit the wider bands of Landsat 8. The 3BDA (KIVU) and 2BDA algorithms were developed with Landsat 7TM bands, so the band math presented here substituted the corresponding Landsat 8 bands (Appendix S1: Table S1). Kab1 and Kab 2 were best-fit algorithms built specifically for low chl *a* coastal use and were included to assess how well a highly specific algorithm might translate to other freshwater regions of study.

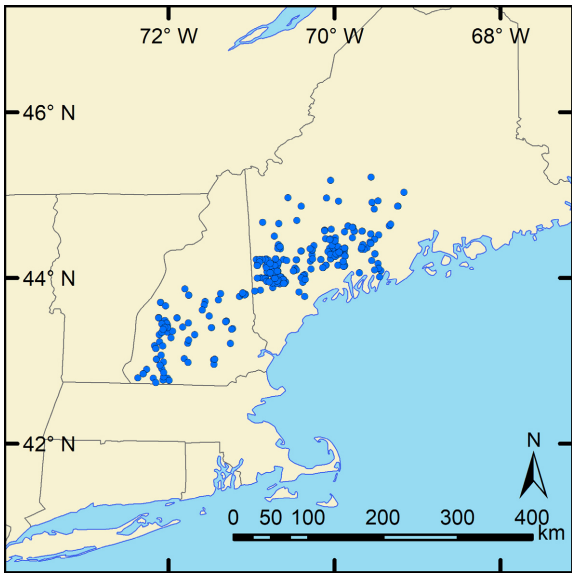

FIG. 1. Locations of in situ chl *a* data from New Hampshire and Maine, USA, lakes corresponding with the scenes listed in Table 1.

The VLAP and VLMP provided exact coordinates for where each in situ sample was taken, and ENVI Geospatial Software was used to process the reflectance output values for each Landsat 8 band at each site. Reflectance values were averaged over a 3 × 3 pixel grid surrounding the sampling point to diminish per-pixel noise. The individual band reflectances could then be combined to find the output in remote-sensing reflectance (Rrs) of each algorithm at each sampling location.

Sensitivity analyses

Region.—The strength of correlations between algorithm output and corresponding in situ chl *a* samples was examined on three different levels of geographic specificity. The broadest analysis of algorithm performance used all chl a samples from both Maine and New Hampshire. We then parsed the analysis by state to assess more specific regional performance of the algorithms. Finally, individual correlations between algorithm output and in situ chl a were calculated for the 19 June 2013, 22 August 2013, and 25 August 2014 Landsat 8 scenes over Maine (Table 5).

Time window.—The 11 Landsat 8 satellite images from Maine and New Hampshire were used for an analysis of the importance of the time window between sample acquisition date and satellite image date. The data set used for each algorithm included either all samples, acquired at most within five days of the satellite image, or the samples that had been acquired within two days. Natural-log-transformed in situ chl a values were plotted against Rrs output for each algorithm and the plots were fitted with linear regression curves. The strength of the correlation for each algorithm was judged using Pearson's r^2 and a P value, where we define a significant relationship as a correlation with $P < 0.05$.

Season.—All of the in situ measurements were categorized into five different chl *a* ranges (0–2.5, 2.5–4, 4–6, 6–10, and

Table 2. Descriptions of each of the six previously published algorithms assessed.

Algorithm	Landsat 8 band math	Original use	Source
Surface Algal Bloom Index (SABI)	(B5 − B4)/(B2 + B3)	ocean, designed to minimize variations in cloud shadow and atmospheric conditions, using MODIS satellite	Alawadi (2010)
3BDA-like (KIVU)	(B2 − B4)/B3	large freshwater lake, above 3 μg/L, Landsat TM	Brivio et al. (2001)
Normalized Difference Vegetation Index (NDVI)	(B5 −B4)/(B5 + B4)	estuarine and coastal waters 1–60 μg/L, using MERIS satellite	Mishra and Mishra (2012)
2BDA	B5/B4	simulated turbid productive freshwater, using Landsat TM	Dall'Olmo and Gitelson (2006)
Kab1	1.67 − 3.94 × ln(B2) + 3.78 × ln(B3)	coastal, best-fit algorithm, chl *a* below 4 μg/L, using Landsat 7	Kabbara et al. (2008)
Kab2	6.92274 − 5.7581 × (ln(B1)/ln(B3))	coastal, best-fit algorithm, chl *a* below 4 μg/L, using Landsat 7	Kabbara et al. (2008)

Notes: The original algorithm band math was converted to the closest comparable Landsat 8 band math. "Original Use" describes the type of water and the satellite for which the algorithm was designed.

≥10 μg/L) and sorted by ordinal day. The algorithm output for samples within each range was plotted against ordinal day in order to assess how algorithm outputs changed with the season for similar in situ samples. Linear models were fitted to each algorithm for each chl a subset to determine the importance of the time of year on the algorithm output.

Model validation

Model validation was conducted to assess the predictive possibilities of the Kab2 algorithm output models. In three Landsat 8 scenes from Maine with cloud cover <15%, 19 June 2013, 22 August 2013 and 25 August 2014, a linear model was built from the algorithm output and natural-log-transformed in situ measurements. The resulting models were applied to the other Maine scenes to calculate predicted natural-log-transformed chl *a*, which were then compared to the in situ measurements to validate the models.

In addition, the two-day Kab2 models built with the 19 June 2013 and 25 August 2014 Maine scenes were validated on a Landsat 7 scene from 26 August 2000 to demonstrate the potential for retroactive chl *a* prediction (Appendix S2: Fig. S1).

Results

All remote sensing algorithms were compared with natural-log-transformed chl *a* in situ data statistically for all scenes and lakes. The results revealed that the Kab1, Kab2, and KIVU algorithm outputs were consistently correlated with natural-log-transformed in situ chl *a* measurements (Table 3). The best performing algorithm was Kab2 with 0.16 correlation coefficient (R^2) and P value of <0.05 when Landsat 8 images within 5 d were used (Fig. 2). The strength of the correlation varied with the specificity of the time window in relation to the in-situ sampling date, explaining up to 27% of the variation (Kab1 and Kab2) in the data across several scenes. The 2BDA, NDVI, and SABI algorithms were not well correlated with natural-log-transformed in situ chl *a*. Additionally, we performed the same analysis on single Landsat 8 scenes using in situ data collected within two days of image acquisition and found a much higher correlation, up to 69% for the 19 June 2013, 22 August 2013, and 25 August 2014 scenes using the Kab2 algorithm. Reducing the time window did not dramatically improve 2BDA, NDVI, or SABI algorithm performance. In general, limiting the chl *a* data set by the time window improved correlations and using one scene at a time showed stronger relationships between satellite outputs and in-situ measurements.

Regional analysis

When all in situ chl *a* data from both Maine and New Hampshire were included (n = 282), Kab1 and Kab2 algorithms performed best, each explaining 15% and 16% of the variation in the data, respectively (Table 3). The KIVU correlation was significant and accounted for 9% of the variation in the data, but none of the other three algorithms had significant correlations. When the chl a data included in the regressions were restricted to the in situ data from Maine (n = 192), Kab1, Kab2, and KIVU algorithm output correlations improved substantially (R^2 = 0.24, 0.25, and 0.18), but the correlations became weaker when only in situ data from New Hampshire (n = 90) were included (R^2 = 0.05, 0.05, and 0.04; Table 4). Correlations with NDVI were significant when New Hampshire and Maine data were considered, but the model explained <10% of the variation (Table 4) in both cases. With 2BDA and SABI, the correlations were slightly stronger in New Hampshire than in Maine, but again no model explained over 10% of variation in chl *a* data.

Table 3. Summary statistics for the linear regression of algorithm output and natural-log-transformed in situ chl *a* measurements.

	5 d of Landsat 8 image			2 d of Landsat 8 image		
Algorithm	R^2	P	RMSE	R^2	P	RMSE
SABI	NS	0.85	NS	NS	0.86	NS
KIVU	0.09	<0.05	0.67	0.17	<0.05	0.69
NDVI	NS	0.08	NS	NS	0.16	NS
2BDA	NS	0.75	NS	NS	0.66	NS
Kab1	0.15	<0.05	0.64	0.27	<0.05	0.65
Kab2	0.16	<0.05	0.64	0.27	<0.05	0.65

Notes: For each of the six algorithms, performance was measured for all in situ data collected within 5 d (n = 282) and 2 d (n = 154) of Landsat 8 image. Correlation coefficients and RMSE values are reported as NS when the relationship was not significant ($P \geq 0.05$).

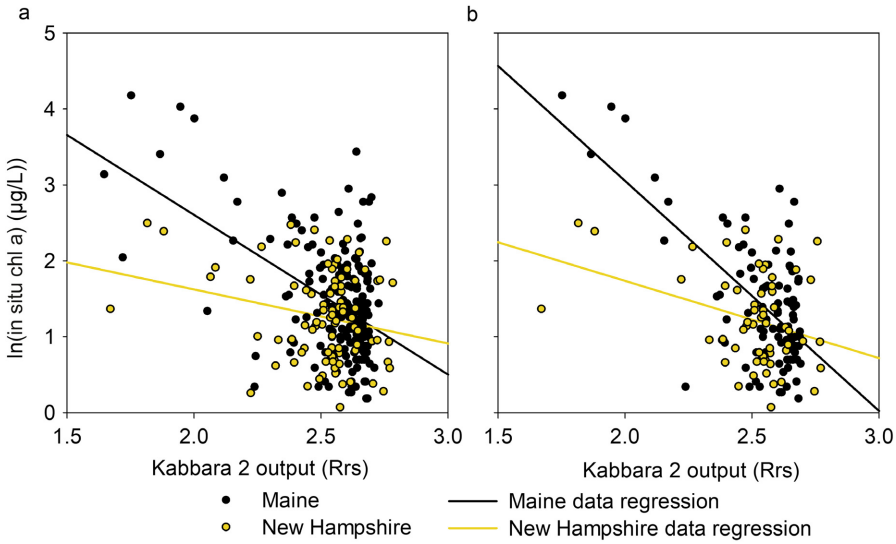

FIG. 2. Correlation between the Kabbara 2 (Kab 2) chl *a* retrieval algorithm output (remote-sensing reflectance, Rrs) and the natural-log-transformed in situ chl *a* (µg/L) measurement for sampling points in Maine and New Hampshire lakes, sampled within 5 d of Landsat 8 image (a, number of Maine points = 192, number of New Hampshire points = 85) or just 2 d of Landsat 8 image (b, number of Maine points = 95, number of New Hampshire points = 59).

Time window analysis

All correlations, on all data, just Maine data, and just New Hampshire data, improved when the chl *a* samples were limited to just those that were collected within two days of the corresponding satellite data. Using data from both regions (n = 154), Kab1, Kab2, and KIVU had significant correlations with r^2 = 0.27, 0.27, and 0.17, respectively. The correlations for 2BDA and SABI were still insignificant (Table 3). With just New Hampshire data (n = 59), all algorithms showed significant correlation, with 2BDA and SABI performing best (r^2 = 0.17, 0.17). All algorithm correlations were significant using just Maine data (n = 95), with Kab1, Kab2, and KIVU performing the best (r^2 = 0.41, 0.43, 0. 31; Table 4).

Single-scene analysis

Restricting the time window to two days and considering only in situ samples in Maine corresponding to a particular Landsat 8 scene produced the strongest correlations (Table 5). There were no significant correlations for the 9 August 2014 Maine scene, but for the other three Maine Landsat 8 scenes, the Kab1, Kab2, and KIVU algorithm outputs accounted for at least 50% of the variation in chl *a*. The strongest correlations were for the 19 June 2013 scene, where Kab1 accounted for 67% and Kab2 69% of chl *a* variation. The NDVI and SABI algorithms were also significantly correlated with chl *a* for all three individual scenes, but never accounted for more than 50% of the variation.

Effect of season

Correlation between ordinal day and all algorithm outputs for specific in situ chl *a* ranges were investigated. Just the results of the best performing algorithm (Kab2) are shown in Fig. 3 for brevity. In this analysis using the Kab2 algorithm, the day of the year explained up to 41% of the variation in algorithm output. For chl *a* between 0 and 2.5 µg/L and between 2.5 and 4 µg/L, the ordinal day had a significant effect on Kab1, Kab2, and KIVU output, but only accounted for between 10% and 16% of variation in algorithm data (not shown here). For chl *a* between 4 and 6 µg/L (n = 55), ordinal day had a significant effect on all six algorithms. It explained <12% of variation for 2BDA, NDVI, and SABI, but over 30% of the variation in algorithm output for Kab1, Kab2, and KIVU (r^2 = 0.31, 0.33, and 0.41). For chl *a* between 6 and 10 µg/L (n = 43), time of year once again had a significant effect on all six algorithms. It explained the most variation for 2BDA, SABI, and KIVU (r^2 = 0.18, 0.18, 0.25) and the least for Kab1 and Kab2 (r^2 = 0.15, 0.14). Finally, for chl *a* over 10 µg/L (n = 24), ordinal day had a significant effect only on 2BDA, NDVI, and SABI algorithm outputs (r^2 = 0.21, 0.21, 0.19).

Model verification

As the best performing algorithm, Kab2 models built using a single scene were tested using another scene with a different acquisition date. Validated on the 25 August 2014 data, the two-day Kab2 model built from the 19 June 2013 scene (M1) explained 57% of variation in chl *a* data with a slope of 0.73, and the model built from the 22 August 2013 scene (M2) explained 67% of variation in chl *a* data with a slope of 0.80 for 19 June 2013 scene. The 19 June 2013 scene and 22 August 2013 scene validated well on one another, but neither model explained more than 10% of the variation in the data from the 9 August 2014 (Table 6).

DISCUSSION

This study aimed to identify a regional model for estimating chl *a* in small, freshwater lakes using Landsat 8 remote sensing technology. Overall, we were able to successfully

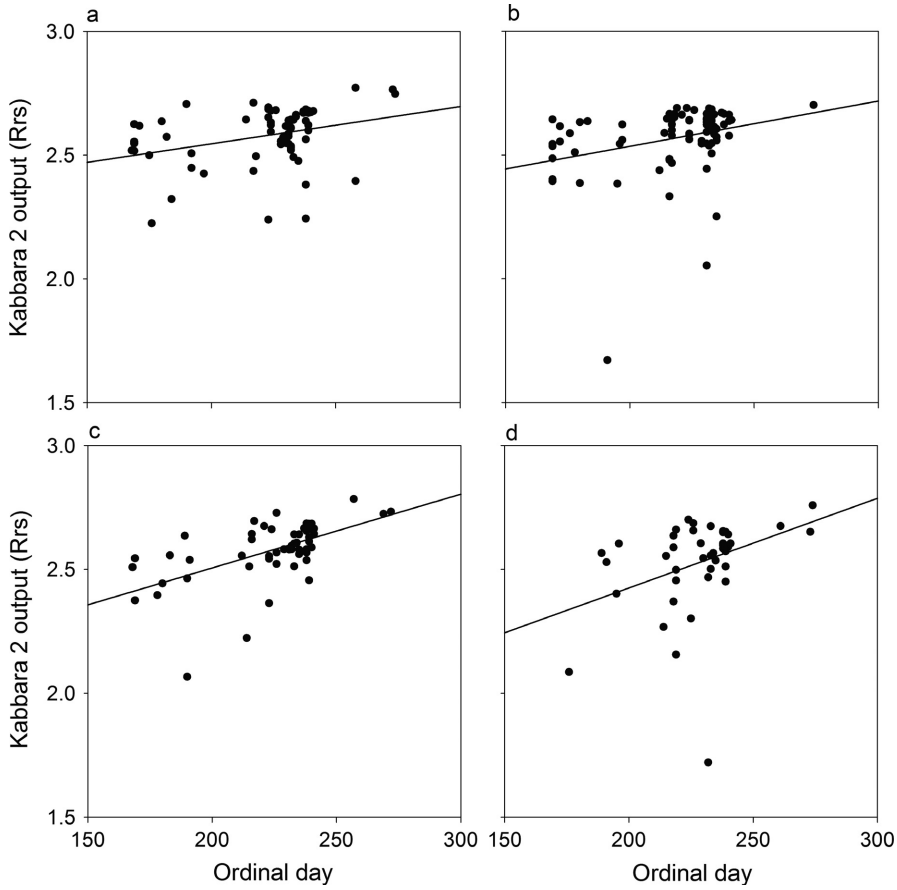

FIG. 3. Correlation between ordinal day and Kab2 algorithm output and specific in situ chl *a* ranges (a, <2.5 μg/L, $n = 75$, $r^2 = 0.11$; b, 2.5–4 μg/L, $n = 83$, $r^2 = 0.11$; c, 4–6 μg/L, $n = 55$, $r^2 = 0.33$; d, 6–10 μg/L, $n = 43$, $r^2 = 0.14$).

model relative concentrations of chl *a* in lakes, of various sizes and across a range of chl *a* concentrations, with moderate degrees of certainty. Thus, the study demonstrated the promising predictive possibility of these models on other Landsat 8 scenes, but identified frequent underprediction of high chl *a* concentrations and difficulty in quantifying low chl a samples, as well as seasonal algorithmic variation.

The relationships between remote-sensing-derived and in situ chl *a* estimates were extremely robust in some cases, but minimal in others. The primary factors affecting the strength of the correlations appear to be the regional scale of analysis, the range of in situ chl *a* values sampled for a particular satellite image, the time window between in situ samples and the satellite image, and the specific algorithm employed.

Regional scale

The strongest correlations between in situ chl *a* and algorithm outputs came when a single Landsat 8 scene was

TABLE 4. Summary statistics for the linear regression of algorithm output and natural-log-transformed in situ chl *a* measurements summarized by state.

	Maine						New Hampshire					
	5 d of Landsat 8 image			2 d of Landsat 8 image			5 d of Landsat 8 image			2 d of Landsat 8 image		
Algorithm	r^2	*P*	RMSE	r^2	*P*	RMSE	r^2	*P*	RMSE	r^2	*P*	RMSE
SABI	0.03	<0.05	0.72	0.11	<0.05	0.79	0.07	<0.05	0.57	0.17	<0.05	0.55
KIVU	0.18	<0.05	0.67	0.31	<0.05	0.69	0.04	<0.05	0.58	0.10	<0.05	0.57
NDVI	0.07	<0.05	0.71	0.15	<0.05	0.77	0.05	<0.05	0.58	0.12	<0.05	0.57
2BDA	0.03	<0.05	0.72	0.10	<0.05	0.80	0.06	<0.05	0.58	0.17	<0.05	0.55
Kab1	0.24	<0.05	0.64	0.41	<0.05	0.64	0.05	<0.05	0.58	0.11	<0.05	0.57
Kab2	0.25	<0.05	0.64	0.43	<0.05	0.63	0.05	<0.05	0.58	0.11	<0.05	0.57

Notes: For each of the six algorithms, performance was measured for all in situ data collected within 5 d (Maine 192 samples, New Hampshire 90 samples) and 2 d (Maine 95 samples, New Hampshire 59 samples) of Landsat 8 image.

TABLE 5. Summary statistics for single-scene algorithm performance.

	6 Jun 2013, $n = 18$			22 Aug 2013, $n = 35$			9 Aug 2014, $n = 15$			25 Aug 2014, $n = 27$		
Algorithm	R^2	P	RMSE	R^2	P	RMSE	R^2	P	RMSE	R^2	P	RMSE
SABI	0.33	<0.05	0.62	0.11	<0.05	0.70	NS	0.11	NS	0.35	<0.05	0.80
KIVU	0.52	<0.05	0.53	0.51	<0.05	0.52	NS	0.19	NS	0.61	<0.05	0.62
NDVI	0.29	<0.05	0.64	0.13	<0.05	0.70	NS	0.11	NS	0.31	<0.05	0.82
2BDA	0.23	<0.05	0.67	NS	0.07	NS	NS	0.12	NS	0.29	<0.05	0.84
Kab1	0.67	<0.05	0.44	0.52	<0.05	0.52	NS	0.31	NS	0.57	<0.05	0.65
Kab2	0.69	<0.05	0.43	0.53	<0.05	0.51	NS	0.25	NS	0.56	<0.05	0.66

Notes: In situ chl *a* data obtained within 2 d of a single Landsat 8 scene were compared against algorithm output resulting in linear models described here. Correlation coefficients and RMSE values are reported as NS when the relationship is not significant ($P \geq 0.05$).

TABLE 6. Summary statistics for the linear regression ($ax + b$) of natural log transformed predicted chl-a (μg/L) vs. natural log transformed in situ chl-*a* (μg/L) using the Kab2 algorithm.

Model name	Scene model built from	Scene model tested on	r^2	P-value	RMSE	a	b	Number of chl-*a* samples used in test
M1	2013-06-19	2013-08-22	0.52	<0.05	0.34	0.48	0.35	35
		2014-08-09	*NA*	0.31	*NA*	*NA*	*NA*	15
		2014-08-25	0.57	<0.05	0.63	0.73	−0.40	27
M2	2013-08-22	2013-06-19	0.67	<0.05	0.35	0.66	0.61	18
		2014-08-09	*NA*	0.31	*NA*	*NA*	*NA*	15
		2014-08-25	0.57	<0.05	0.69	0.80	−0.21	27
M3	2014-08-25	2013-06-19	0.67	<0.05	0.25	0.47	1.36	18
		2013-08-22	0.52	<0.05	0.27	0.37	1.26	35
		2014-08-09	*NA*	0.31	*NA*	*NA*	*NA*	15

Notes: Models were built using Kab2 output of a single scene (Scene model built from) vs. measured natural log transformed chl-*a* sampled within 2 d of image acquisition. Models were then tested on data from another single Maine Landsat 8 scene ('Scene model tested on'). Correlation coefficients, RMSE, slope and intercept values are reported as NA when the relationship is not significant ($P \geq 0.05$).

analyzed (Table 5). These scenes each covered over 12,000 m^2 of land, thus still providing a useful regional model, and the Kab1, Kab2, and KIVU algorithms consistently accounted for over one-half of the variation in chl *a*. Compared to previous studies that focused on remote sensing applications to specific areas (Kabbara et al. 2008, Moses et al. 2012, Tebbs et al. 2013, Watanabe et al. 2015, Ho et al. 2017, Liga et al. 2017), robust models built for the dozens of lakes within even a single Landsat 8 scene represent an improvement in regional applicability of retrieval algorithms. Considering the diversity of lake characteristics included within our most narrow regional analysis, the success of the Kab1 and Kab2 algorithms in particular is a good sign for large-scale sorting of lakes by trophic state with remote sensing technology.

More general subsets of data that separated chl *a* samples by state showed inconsistent results, and application of the algorithms to lakes from both states accounted at best for 16% of the variation in chl *a* (Fig. 2). The stark differences between the robust correlations in Maine and the weaker relationships in New Hampshire are possibly attributable to the fact that the Maine lakes had a range of chl *a* concentrations, whereas New Hampshire had nearly all samples with chl $a < 10$ μg/L. Even for the Maine scenes, algorithm outputs for low chl *a* lakes were scattered, but the outputs for the higher chl *a* samples were more distinct, suggesting that developing models aimed at algal bloom identification requires inclusion of as many high chl *a* samples as possible.

While differences in sampling technique between New Hampshire and Maine and even individual volunteer organizations (depth of sample, core vs. grab) could be the source of distinct different performances of remote sensing algorithms, we think it is unlikely that sampling differences would result in much higher or lower in situ chl a data and thus may not be a large source of error. The difference in acquisition time between satellite data and the lakes from two regions as well as uncertainty in precise location of sampling of each lake may also explain some of the variance in the algorithms.

Time window

Decreasing the time between the measured chl *a* concentration and the satellite image consistently improved algorithm performance (Tables 3 and 4). The inconsistent distribution of samples around each scene made a rigorous analysis in regard to a minimum acceptable time window difficult, but it was evident that the most robust algorithms are those where in situ and remote sensing sampling are matched in time. This finding is consistent with previous studies (Kabbara et al. 2008, Keith et al. 2012, Urbanski et al. 2016). Spatial heterogeneity in phytoplankton distribution within a lake as well as weather events/changes such as wind or rain events, besides actual changes in phytoplankton density and distribution that occur between the in situ sample and the satellite image acquisition times can

increase the uncertainty of the algorithm outputs (Toming et al. 2016).

Algorithms

The KIVU, Kab1, and Kab2 algorithms, which used Landsat 8 Bands 1–4 and not Band 5 as in 2BDA, SABI, and NDVI, consistently demonstrated the strongest relationships with in situ chl *a*. Derived combinations of bands 1–4 like those used by Kabbara et al. (2008) were designed for prediction within a specific region and season, but the success of Kab1 and Kab2 in this study suggest that these complex algorithms are useful outside of the original area of study. The 2BDA, SABI, and NDVI algorithms have proved effective retrieval algorithms using satellites other than Landsat 8 because of the narrower near-infrared band (NIR). Landsat 8's NIR Band 5, however, is the closest comparable band with wavelength of 850–880 nm. This is well over the 706 nm wavelength absorbance peak of chl *a*, which is more accurately represented in NDVI and NDCI (normalized difference chlorophyll index) remote sensing indices using other satellites (Mishra and Mishra 2012).

Although the three algorithms that did not use Band 5 performed much better in general, the algorithms that did incorporate this band appeared to be slightly better suited for monitoring low chl a lakes. The 2BDA, NDVI, and SABI algorithms, which used this Band 5, typically performed better on New Hampshire chl *a* data compared to Maine or all data. In fact, for New Hampshire data collected within two days of image acquisition, these three algorithms actually outperformed the others. Because the key difference between the New Hampshire data and Maine data was the absence of chl *a* samples above 10 μg/L, these results suggest that Landsat 8's Band 5 may be useful for chl *a* monitoring in regions with mainly oligotrophic lakes. Previous work with other satellites identified blue/green ratios as most applicable to retrieve 0–10 μg/L chl *a* concentrations and red-NIR ratios for higher chl *a* concentrations (Odermatt et al. 2012), but Landsat 8's NIR band placement well beyond the chl *a* absorbance peak likely affects this relationship. An optimal algorithm might thus need to incorporate reflectance data from more than just two or three Landsat bands to be applicable to lakes with a wide range of trophic states.

Cloud cover and corrections

All scenes in this study were selected specifically to have below 20% cloud cover, and no sampling point near a cloud was included, however, there was evidence that cloud cover affected within-scene algorithm performances. In New Hampshire, only one of the four summer scenes (3 August 2015) had cloud cover below 5%, and the correlations between algorithm outputs and chl *a* were strongest on this date. In Maine, the 19 June 2013 and 25 August 2014 scenes had below 5% cloud cover and also had the strongest correlations. In contrast, the 9 August 2014 scene had 16% cloud cover, the highest for a Maine scene, and very weak correlations.

It should be noted that the dark object subtraction (DOS), which we used, is a relatively quick and simple method for atmospheric correction in this analysis and more vigorous atmospheric correction methods should be examined in the future. The cloud interference can cause lowering of the signal-to-noise ratio of reflectances, especially in blue and green bands (Bands 2 and 3), which could be problematic for detecting low chl *a* concentrations. More comprehensive atmospheric corrections may alleviate the issue of detecting low chl *a* events. Mishra and Mishra (2012) noted that MERIS satellite images that were not cloud-free required cloud masking before effectively interpreting chl *a* retrieval algorithm data. Urbanski et al.'s (2016) study in Poland relied on uncloudy images too, and concluded that at least in the region of their study, Landsat 8 and the European Space Agency's Sentinal 2 satellite would together provide at least one uncloudy image each month. Current investigations of atmospheric correction techniques for Landsat 8 are aiming to reduce the weather limitations of remote sensing so that some cloud presence in an image can still produce robust chl *a* prediction results (Concha and Schott 2015). Concha and Schott (2015) performed an analysis to quantify the effect of atmospheric corrections on several models and proposed a look-up-table using a Hydrolight model, which could be used for improving the detection of low chl *a* lakes.

Effect of season

The effect that the time of year had on algorithm outputs depended on both the algorithm and the chl *a* range considered, but the data in many cases suggested a nontrivial effect of time of year on algorithm output. The KIVU, Kab1, and Kab2 algorithms were all significantly affected by season for the *lowest* four chl *a* ranges. The strongest effects were observed in the 6–10 μg/L category, followed by the 4–6 μg/L (Fig. 4). On the other hand, the 2BDA, SABI, and NDVI algorithms were significantly affected by season only for the *highest* three chl *a* ranges and the effect was strongest for the ≥10 μg/L category. This grouping of algorithms is the same as discussed above, with the distinguishing factor again being the use of Landsat 8's red Band 4 and NIR Band 5. These effect-of-season results suggest not only that algorithms may need to be tuned by season, but also that certain bands may be subject to more seasonal variation than others depending on the types of lakes in question.

This seasonal specificity poses a challenge for predictive remote sensing, which would ideally be tuned specifically to chl *a* so that seasonal variation in other water quality parameters does not affect the output. Liga et al. (2017) suggested that changing composition of phytoplankton assemblages throughout the year would change the optical properties of blooms enough to warrant season-specific algorithms for particular regions. Despite the limitations imposed by Landsat 8's relatively narrow bands, Landsat 8's thermal Bands 10 and 11 are relatively well correlated with surface water temperature (data not included), and could potentially be incorporated into chl *a* retrieval algorithms as a seasonal correction term.

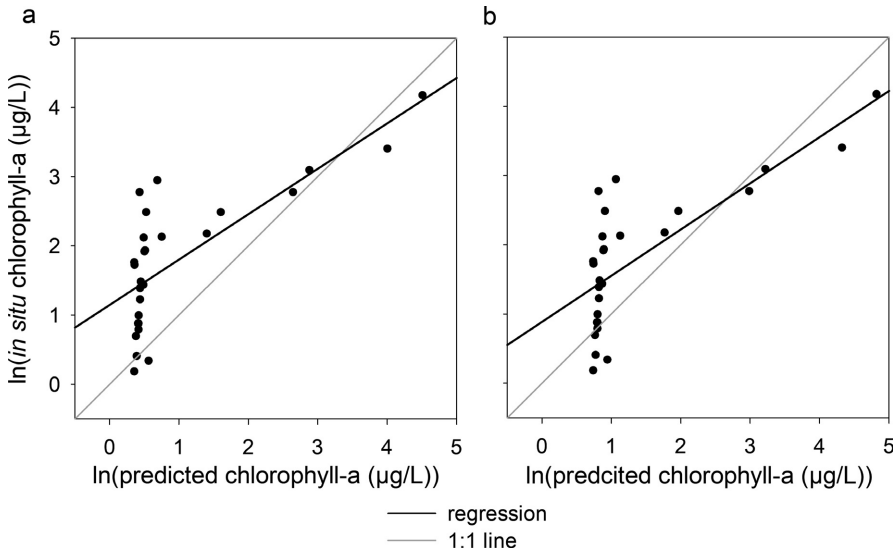

FIG. 4. Predicted natural-log-normal values of chl a for scene from 25 August 2014 (n =27) vs natural-log-transformed in situ measurements using (a) M1 based on 19 June 2013 scene, $r^2 = 0.57$, $P < 0.05$, RMSE = 0.63, slope = 0.73, y intercept = −0.40, and (b) M2 based on 22 August 2013 scene, $r^2 = 0.57$, $P < 0.05$, RMSE = 0.69, slope = 0.80, y intercept = −0.21.

Predictive potential and future work

The regional correlations between chl *a* retrieval algorithms and in situ samples across hundreds of lakes in northern New England represents an important advance in the application of remote sensing technology. Such correlations will ideally be used to develop models built on one or several satellite scenes to accurately predict chl *a* from other scenes acquired in the future. The validation results from this study clearly indicate that this type of prediction is possible even when many different lakes are in question. With the exception of one validation scene (Table 6), the models we developed categorized water bodies by chl *a* with moderate accuracy (Fig. 4). The validation slopes consistently <1 suggested underestimation of chl *a* and highlighted the importance of including as many high chl *a* samples as possible in the data used to make the predictive models. The models also clearly had difficulty resolving the low chl a samples; there was a plateau once chl *a* was below 2 µg/L. This is similar to the 3 µg/L sensitivity limit described by Brivio et al. (2001) using the KIVU algorithm, but Kabbara et al. (2008) found that the Kab1 and Kab2 algorithms explained >70% of the variation in 34 chl *a* samples below 4 µg/L in coastal Tripoli, so there is evidence that low chl *a* detection may be possible with algorithms finely tuned by region.

Even though the Kab2 linear correlation models do not predict the actual chl *a* concentration within a narrow margin of error, differentiation between classes of lakes is useful, especially on a regional scale. Recent studies for large-scale remote sensing have been satisfied with simply classifying the trophic status of lakes into broad categories (Bresciani et al. 2011, Watanabe et al. 2015, Urbanski et al. 2016). In a region like the Northeastern United States, remotely sensed classification of the hundreds of lakes in the area would be a powerful tool for water quality management.

We found initial evidence for the applicability of modern chl *a* retrieval models to retroactive investigations of chl *a* analysis from archived satellite images from previous Landsat iterations. A Landsat 7 image from 26 August 2000 was selected for its low cloud cover (0.31%) and the availability of local in situ chl *a* data from within two days. Use of the Kab1 model demonstrated clear categorization of the chl *a* samples from low to high (Appendix S2: Fig. S1). The Kab1 algorithm was chosen for this analysis because Landsat 7 does not have a band correlative to Landsat 8's Band 1, which is required for the Kab2 algorithm, and, in general, the Kab1 models showed comparable results to Kab2. The backward time-series applicability of predictive chl *a* models was recently also demonstrated in a case study of Lake Erie algal blooms using Landsat data (Ho et al. 2017). This potential deserves further investigation. Both the Landsat archives and many water monitoring databases hold vast amounts of valuable historical data that could be combined to estimate chl a concentrations in a region across several decades.

SUMMARY AND CONCLUSIONS

Here we compared in situ chl *a* concentration measurements to chl a retrieval algorithm predictions from satellite observations over Maine and New Hampshire. The KIVU, Kab1, and Kab2 algorithms in particular, which used Landsat 8 bands 1–4 rather than band 5, explained large amounts of the variation in measured vs. predicted chl *a*. The correlations were highest on days with minimum amount of cloud, and improved dramatically with increased temporal coincidence of the sampling effort as well as increased specificity of the geographic distribution of data. The seasonal variation in the algorithm outputs suggests the need for specific seasonal algorithm tuning, but the effects can also likely be mitigated with strategic band choice depending on the lakes in question and incorporation of remotely sensed water temperature in lieu of narrower satellite bands. The validation results showed that models built using a wide enough range

of sampled concentrations can, in some cases, reliably classify the chl *a* concentration in any given 30-m pixel in past or future satellite images that is cloud-free.

This investigation points to improvements that both remote sensing specialists and freshwater scientists could make to advance large scale remote sensing of freshwater resources. First, the coordination of sampling efforts with satellite overpasses would provide much more data for model development. Samples nearly coincident with the satellite image are clearly more useful for investigating correlations and building predictive models. Second, the application of remote sensing to solving ecological problems will require intentional band design to maximize the ecological relevance of reflectance outputs. This study confirms Beck et al.'s (2016) conclusion that high spatial resolution satellites like Sentinal-2 and Landsat 8 are most relevant for monitoring small inland water bodies even though they sacrifice the spectral resolution that other satellites offer. As engineers continue to weigh the trade-offs between temporal resolution, spatial resolution, and spectral resolution, it will be important to take into account the needs of end users such as scientists, managers, and policy makers.

Acknowledgments

We thank Dr. Satya Prakash, as well as Saba Saberi and Jaelyn Bos for technical assistance. This research was funded, in part, through an NSF-REU site program (NSF 1559769), and an NSF Macrosystems Biology grant (EF-113732) and the Cary Institute's G. Evelyn Hutchinson Chairship.

Literature Cited

Alawadi, F. 2010. Detection of surface algal blooms using the newly developed algorithm surface algal bloom index (SABI). Proceedings of the International Society for Optics and Photonics 7825:1–14.

Beck, R., et al. 2016. Comparison of satellite reflectance algorithms for estimating chlorophyll-a in a temperate reservoir using coincident hyperspectral aircraft imagery and dense coincident surface observations. Remote Sensing of Environment 178:15–30.

Bresciani, M., D. Stroppiana, D. Odermatt, G. Morabito, and C. Giardino. 2011. Assessing remotely sensed chlorophyll-a for the implementation of the Water Framework Directive in European perialpine lakes. Science of the Total Environment 409:3083–3091.

Brivio, P. A., C. Giardino, and E. Zilioli. 2001. Determination of chlorophyll concentration changes in Lake Garda using an image-based radiative transfer code for Landsat TM images. International Journal of Remote Sensing 22:487–502.

Carey, C. C., K. C. Weathers, and K. L. Cottingham. 2009. Increases in phosphorus at the sediment-water interface may influence the initiation of cyanobacterial blooms in an oligotrophic lake. International Association of Theoretical and Applied Limnology: Negotiations 30:1185–1188.

Concha, J. A., and J. R. Schott. 2015. Atmospheric correction for Landsat 8 over case 2 waters. Earth Observing Systems XX 9607:96070R.

Concha, J. A., and J. R. Schott. 2016. Retrieval of color producing agents in Case 2 waters using Landsat 8. Remote Sensing of Environment 185:95–107.

Dall'Olmo, G., and A. A. Gitelson. 2006. Effect of bio-optical parameter variability and uncertainties in reflectance measurements on the remote estimation of chlorophyll-a concentration in turbid productive waters: modeling results. Applied Optics 45:3577–3592.

Davis, R. B., D. S. Anderson, S. S. Dixit, P. G. Appleby, and M. Schauffler. 2006. Responses of two New Hampshire (USA) lakes to human impacts in recent centuries. Journal of Paleolimnology 35:669–697.

Dörnhöfer, K., and N. Oppelt. 2016. Remote sensing for lake research and monitoring - recent advances. Ecological Indicators 64:105–122.

Duan, H., Y. Zhang, B. Zhang, K. Song, and Z. Wang. 2007. Assessment of chlorophyll-a concentration and trophic state for Lake Chagan using Landsat TM and field spectral data. Environmental Monitoring and Assessment 129:295–308.

Feyisa, G. L., H. Meilby, R. Fensholt, and S. R. Proud. 2014. Automated Water Extraction Index: a new technique for surface water mapping using Landsat imagery. Remote Sensing of Environment 140:23–35.

Gerace, A. D., J. R. Schott, and R. Nevins. 2013. Increased potential to monitor water quality in the near-shore environment with Landsat's next-generation satellite. Journal of Applied Remote Sensing 7:73558.

Giardino, C., M. Pepe, P. A. Brivio, P. Ghezzi, and E. Zilioli. 2001. Detecting chlorophyll, Secchi disk depth and surface temperature in a sub-alpine lake using Landsat imagery. Science of the Total Environment 268:19–29.

Hanson, P. C., K. C. Weathers, and T. K. Kratz. 2016. Networked lake science: How the Global Lake Ecological Observatory (GLEON) works to understand, predict, and communicate lake ecosystem response to global change. Inland Waters 6:543–554.

Ho, J. C., R. P. Stumpf, T. B. Bridgeman, and A. M. Michalak. 2017. Using Landsat to extend the historical record of lacustrine phytoplankton blooms: a Lake Erie case study. Remote Sensing of Environment 191:273–285.

Kabbara, N., J. Benkhelil, M. Awad, and V. Barale. 2008. Monitoring water quality in the coastal area of Tripoli (Lebanon) using high-resolution satellite data. ISPRS Journal of Photogrammetry and Remote Sensing 63:488–495.

Keith, D. J., B. Milstead, H. Walker, H. Snoo, J. Szykman, M. Wusk, L. Kagey, C. Howell, C. Mellanson, and C. Drueke. 2012. Trophic status, ecological condition, and cyanobacteria risk of New England lakes and ponds based on aircraft remote sensing. Journal of Applied Remote Sensing 6:063577.

Liga, M., T. Kutser, K. Kallio, J. Attila, S. Koponen, B. Paavel, T. Soomets, and A. Reinart. 2017. Testing the performance of empirical remote sensing algorithms in the Baltic Sea waters with modelled and *in situ* reflectance data. Oceanologia 509: 57–68.

Maine Volunteer Lake Monitoring Program. 2017. http://www.mainevlmp.org/about/.

Mishra, S., and D. R. Mishra. 2012. Normalized difference chlorophyll index: a novel model for remote estimation of chlorophyll-a concentration in turbid productive waters. Remote Sensing of Environment 117:394–406.

Moore, T. S., M. D. Dowell, S. Bradt, and A. Ruiz Verdu. 2014. An optical water type framework for selecting and blending retrievals from bio-optical algorithms in lakes and coastal waters. Remote Sensing of Environment 143:97–111.

Moses, Wesley. J., A. A. Gitelson, S. Berdnikov, V. Saprygin, and V. Povazhnyi. 2012. Operational MERIS-based NIR-red algorithms for estimating chlorophyll-a concentrations in coastal waters—The Azov Sea case study. Remote Sensing of Environment 121:118–124.

New Hampshire Department of Environmental Services. 2015. Annual Report. http://www.des.nh.gov/organization/divisions/water/wmb/vlap/.

Odermatt, D., A. Gitelson, V. E. Brando, and M. Schaepman. 2012. Review of constituent retrieval in optically deep and complex waters from satellite imagery. Remote Sensing of Environment 118:116–126.

Palmer, S. C. J., T. Kutser, and P. D. Hunter. 2015. Remote sensing of inland waters: challenges, progress and future directions. Remote Sensing of Environment 157:1–8.

Roy, D. P., et al. 2014. Landsat-8: science and product vision for terrestrial global change research. Remote Sensing of Environment 145:154–172.

Schloss, A. L., S. Spencer, J. A. Schloss, J. Haney, S. Bradt, and J. Nowak. 2002. Using Landsat TM data to aid the assessment of long-term trends in lake water quality in New Hampshire lakes. Geoscience and Remote Sensing Symposium 00:3095–3098.

Shen, L., H. Xu, and X. Guo. 2012. Satellite remote sensing of harmful algal blooms (HABs) and a potential synthesized framework. Sensors (Switzerland) 12:7778–7803.

Stoddard, John. L., J. V. Sickle, A. T. Herlihy, J. Brahney, S. Paulsen, D. V. Peck, R. Mitchell, and A. I. Pollard. 2016. Continental-scale increase in lake and stream phosphorous: Are oligotrophic systems disappearing in the United States? Environmental Science and Technology 50:3409–3415.

Tebbs, E. J., J. J. Remedios, and D. M. Harper. 2013. Remote sensing of chlorophyll-a as a measure of cyanobacterial biomass in Lake Bogoria, a hypertrophic, saline-alkaline, flamingo lake, using Landsat ETM+. Remote Sensing of Environment 135:92–106.

Toming, K., T. Kutser, A. Laas, M. Sepp, B. Paavel, and T. Nõges. 2016. First experiences in mapping lake water quality parameters with Sentinel-2 MSI imagery. Remote Sensing 8:640.

Urbanski, J. A., A. Wochna, I. Bubak, W. Grzybowski, K. Lukawska-Matuszewska, M. Łącka, S. Śliwińska, B. Wojtasiewicz, and M. Zajączkowski. 2016. Application of Landsat 8 imagery to regional-scale assessment of lake water quality. International Journal of Applied Earth Observation and Geoinformation 51:28–36.

U.S. EPA (Environmental Protection Agency). 2010. Using remote sensing to monitor water quality in New England lakes (pp. 35–38). Gauging the health of New England's lakes and ponds: a survey report and decision-making resource (October 10). U.S. EPA, Washington, D.C., USA.

U.S. Geological Survey, National Geospatial Program. 2017*a*. USGS National Hydrography Dataset (NHD) Best Resolution 20170714 for Maine State or Territory FileGDB 10.1 Model in Version 2.2.1. U.S. Geological Survey, Reston, Virginia, USA.

U.S. Geological Survey, National Geospatial Program. 2017*b*. USGS National Hydrography Dataset (NHD) Best Resolution 20170714 for New Hampshire State or Territory FileGDB 10.1 Model Version 2.2.1. U.S. Geological Survey, Reston, Virginia, USA.

Vertucci, F. A., and G. E. Likens. 1989. Spectral reflectance and water quality of Adirondack mountain region lakes. Limnology and Oceanography 34:1656–1672.

Watanabe, F. S., E. Alcântara, T. W. Rodrigues, N. N. Imai, C. C. Barbosa, and L. H. Rotta. 2015. Estimation of chlorophyll-a concentration and the trophic state of the barra bonita hydroelectric reservoir using OLI/Landsat-8 images. International Journal of Environmental Research and Public Health 12:10391–10417.

Supporting Information

Additional supporting information may be found online at: http://onlinelibrary.wiley.com/doi/10.1002/eap.1708/full

Data Availability

Data available from the Environmental Data Initiative (EDI) Data Portal: https://doi.org/10.6073/pasta/c9ef66c8c192fb73086ea08c8d7a00ff